

Adrian Jonas, Steffen Staeck, Birgit Kanngießer, Holger Stiel, Ioanna Mantouvalou

Laboratory quick near edge x-ray absorption fine structure spectroscopy in the soft x-ray range with 100 Hz frame rate using CMOS technology

Open Access via institutional repository of Technische Universität Berlin

Document type

Journal article | Published version

(i. e. publisher-created published version, that has been (peer-) reviewed and copyedited; also known as: Version of Record (VOR), Final Published Version)

This version is available at

<https://doi.org/10.14279/depositonce-15602>

Citation details

This article may be downloaded for personal use only. Any other use requires prior permission of the author and AIP Publishing. This article appeared in

Jonas, A., Staeck, S., Kanngießer, B., Stiel, H., & Mantouvalou, I. (2021). Laboratory quick near edge x-ray absorption fine structure spectroscopy in the soft x-ray range with 100 Hz frame rate using CMOS technology. In Review of Scientific Instruments (Vol. 92, Issue 2, p. 023102). AIP Publishing.
and may be found at <https://doi.org/10.1063/5.0032628>.

Terms of use

This work is protected by copyright and/or related rights. You are free to use this work in any way permitted by the copyright and related rights legislation that applies to your usage. For other uses, you must obtain permission from the rights-holder(s).

Laboratory quick near edge x-ray absorption fine structure spectroscopy in the soft x-ray range with 100 Hz frame rate using CMOS technology

Cite as: Rev. Sci. Instrum. **92**, 023102 (2021); <https://doi.org/10.1063/5.0032628>

Submitted: 12 October 2020 • Accepted: 24 January 2021 • Published Online: 16 February 2021

 Adrian Jonas, Steffen Staeck,  Birgit Kanngießer, et al.



View Online



Export Citation



CrossMark

ARTICLES YOU MAY BE INTERESTED IN

Attosecond state-resolved carrier motion in quantum materials probed by soft x-ray XANES



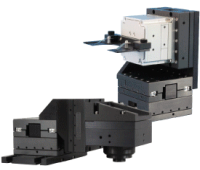
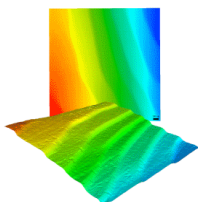
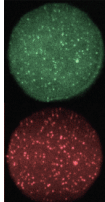
Applied Physics Reviews **8**, 011408 (2021); <https://doi.org/10.1063/5.0020649>

High-resolution inelastic x-ray scattering at the high energy density scientific instrument at the European X-Ray Free-Electron Laser

Review of Scientific Instruments **92**, 013101 (2021); <https://doi.org/10.1063/5.0022886>

Determining the water content of nominally anhydrous minerals at the nanometre scale

Review of Scientific Instruments **92**, 023103 (2021); <https://doi.org/10.1063/5.0025570>

 MCL MAD CITY LABS INC. www.madcitylabs.com	<p>Nanopositioning Systems</p> 	<p>Modular Motion Control</p> 	<p>AFM and NSOM Instruments</p> 	<p>Single Molecule Microscopes</p> 
---	--	--	---	--

Laboratory quick near edge x-ray absorption fine structure spectroscopy in the soft x-ray range with 100 Hz frame rate using CMOS technology

Cite as: Rev. Sci. Instrum. 92, 023102 (2021); doi: 10.1063/5.0032628

Submitted: 12 October 2020 • Accepted: 24 January 2021 •

Published Online: 16 February 2021



Adrian Jonas,^{1,2,a)} Steffen Staeck,^{1,2} Birgit Kanngießner,^{1,2} Holger Stiel,^{1,3} and Ioanna Mantouvalou^{1,2,b)}

AFFILIATIONS

¹Berlin Laboratory for Innovative X-ray Technologies (BLIX), D-10623 Berlin, Germany

²TU Berlin, Analytical X-Ray Physics, D-10623 Berlin, Germany

³Max-Born-Institut für Nichtlineare Optik und Kurzzeitspektroskopie, D-12489 Berlin, Germany

^{a)} Author to whom correspondence should be addressed: Adrian.Jonas@campus.tu-berlin.de

^{b)} Current address: Helmholtz Zentrum Berlin, D-12489, Germany.

ABSTRACT

In laboratory based x-ray absorption fine structure (XAFS) spectroscopy, the slow readout speed of conventional CCD cameras can prolong the measuring times by multiple orders of magnitude. Using pulsed sources, e.g., laser-based x-ray sources, the pulse repetition rate often exceeds the frame rate of the CCD camera. We report the use of a scientific CMOS (sCMOS) camera for XAFS spectroscopy with a laser-produced plasma source facilitating measurements at 100 Hz. With this technological improvement, a new class of experiments becomes possible, starting from the time consuming analysis of samples with small absorption to pump-probe investigations. Furthermore, laboratory quick soft x-ray absorption fine structure (QXAFS) measurements with 10 ms time resolution are rendered feasible. We present the characterization of the sCMOS camera concerning noise characteristics and a comparison to conventional CCD camera performance. The feasibility of time resolved QXAFS measurements is shown by analyzing the statistical uncertainty of single shot spectra. Finally, XAFS spectroscopy on a complex sandwich structure with minute amounts of NiO exemplifies the additional merits of fast detectors.

Published under license by AIP Publishing. <https://doi.org/10.1063/5.0032628>

I. INTRODUCTION

X-ray absorption fine structure (XAFS) spectroscopy is an analytical tool for the investigation of the element specific electronic structure of atoms or molecules inside a sample. In quick x-ray absorption fine structure (QXAFS) measurements, absorption spectra are taken in quick succession to resolve dynamical processes in the millisecond to minute range.^{1–10} The technique is a powerful tool for investigating *in situ* reactions and slow dynamic processes. XAFS is currently most commonly performed at synchrotron radiation facilities due to the available high flux and efficient instrumentation. For measurements, the excitation energy is scanned in the region of the probed absorption edge and absorption is measured via transmission, fluorescence, or electron detection. For QXAFS measurements, only synchrotron radiation experiments have been presented up until now, with a focus on hard x rays and

the extended XAFS (EXAFS) region and limited applications in the soft x-ray regime.^{11,12}

In the laboratory, x-ray sources are invariably less brilliant, which triggered the use of scan-free approaches for XAFS, where the polychromatic excitation radiation is first transmitted through a sample and then detected with wavelength dispersive instrumentation. Today, soft XAFS setups in the laboratory use light from high harmonic generation sources^{13–18} or laser-produced plasma (LPP) sources^{19–21} together with dispersive optics and position sensitive detectors. In all published cases, a large area CCD sensor is used to collect the spatially separated photons. CCD sensors show a high sensitivity in the soft x-ray region, a very low noise level, and a large active sensor area, which is crucial for a high spectral resolving power and bandwidth. The downside of these large CCD sensors is the readout time, which ranges from hundreds of milliseconds to seconds. These readout times can prolong

the measuring times by multiple orders of magnitude if single shot measurements are advantageous or mandatory and would result in a time resolution of seconds for QXAFS investigations.²² Advances of laser-based laboratory soft x-ray sources with repetition rates of 100 Hz to MHz call for detectors that can reach equal frame rates. Electron-multiplying CCDs or pn-CCD cameras manage the high repetition rates but show an inadequate image area or pixel size, limiting either the energy range or energy resolution of the measured XAFS spectra.

CMOS sensors are used in numerous scientific and non-scientific applications ranging from consumer electronics to space missions.²³ For most applications, front-illuminated cameras are used, which are equipped with microlens arrays to improve the sensitivity in the visible spectral range. For the detection of soft x-rays, CCD cameras still find widespread use and only recently suitable CMOS camera chips are becoming available.^{24–26} One of the key differences between common CMOS and CCD cameras is that a CCD sensor has only one readout unit, while in a CMOS detector each pixel or each pixel row converts the electrons into voltage and amplifies it individually. This leads to much higher readout rates at the cost of additional noise contributions in CMOS detectors. Due to multiple amplifiers, the dark signal non-uniformity (DSNU), defined as the temporal noise adjusted standard deviation of the pixel base values, and the pixel response non-uniformity (PRNU), which describes the standard deviation of the pixel gain, must be taken into account for CMOS detectors. Very recently, back-illuminated 16-bit scientific CMOS (sCMOS) sensors without on-chip microlenses became commercially available and were characterized regarding energy and spatial resolution, noise level, and soft x-ray quantum efficiency^{24–27} with results showing the potential of sCMOS cameras for soft x-ray applications.

In this article, we present measurements regarding the noise and gain values of a modified Tucsen Dhyana 95 sCMOS camera, which are crucial when measuring small signals. Using a laboratory XAFS setup based on a laser-produced plasma source operating at a repetition rate of 100 Hz, a reduced acquisition time compared to the use of a standard CCD camera is presented. The ability to perform QXAFS measurements with up to 10 ms time resolution is demonstrated and discussed. Finally, a sandwich sample with very low absorption at the Ni L edge is investigated demonstrating the advantages of high speed soft x-ray cameras.

II. EXPERIMENTAL

A. Scientific CMOS and CCD camera

The camera used is the commercially available Tucsen Dhyana 95 V1 with a 4 MPixel (2048 × 2048) resolution, a chip size of 22.5 × 22.5 mm², and a pixel size of 11 × 11 μm². The sCMOS is based on the back-illuminated GSENSE400BSI sensor by GPIXEL Inc., with the quantum efficiency increasing from 0.3 eV at 284 eV (C K-edge) to 0.8 at 1303 eV (Mg K-edge).²⁵ It can be cooled down to −20 °C using a Peltier element and air cooling. Using the full frame and 16-bit pixel values, the camera can collect 24 frames per second (fps). The camera has readout electronics for each pixel row, so by choosing a fragmentary number of rows to be read out, the frame rate can be increased. If a cutout with 460 rows or less is selected,

100 fps can be reached. The camera offers two measurement modes, the High Gain (HG) mode and High Dynamic Range (HDR) mode, the former using a higher gain and lower dynamic range compared to the latter.

The sCMOS camera is designed for visible light and is equipped with an entrance window and commonly with an anti-reflection coating on the chip. To be used for soft x-ray detection, the entrance window was removed and an ISO-K 160 flange was attached on the front side of the camera. The modified camera is depicted in Fig. 1.

The used CCD camera is the GE 2048 2048 from Greateyes GmbH.²⁸ Its back-illuminated chip is 27.6 × 27.6 mm² large and has a pixel size of 13.5 × 13.5 μm². The quantum efficiency ranges from 0.65 at 284 eV (C K-edge) to 0.8 at 1303 eV (Mg K-edge). The gain is 1 count/e[−], and the full well capacity is 100 ke[−]. At −20 °C and 1 MHz readout speed (0.25 fps), the camera features a readout noise of 8.5 e[−] and a dark noise of 1 e[−]/pixel/s.

B. Experimental setup

In this work, a laser-produced plasma (LPP) was used as the source of soft x-ray radiation. The source is explained in detail in Ref. 29. Briefly, the LPP consists of a Yb:YAG thin disk laser with a repetition rate of 100 Hz and a solid state metal target. A laser pulse with a wavelength of 1030 nm and a pulse energy of up to 200 mJ is focused onto a rotating cylinder with a changeable target material (typically Cu or W), which forms a hot dense plasma with a size in the range of 50 μm (FWHM). The pulse duration can be continuously varied between 0.5 ns and 30 ns. The plasma emits polychromatic and isotropic radiation in the range of 100 eV–1600 eV. A photograph of the setup is shown in Fig. 2.

The XAFS measurements were performed using a twin-arm reflection zone plate spectrometer previously described in Ref. 22. The sample is measured in transmission mode, and the incident x-ray spectrum is collected simultaneously using a pair of off-axis reflection zone plate optics. A 200 nm thick Al filter blocks

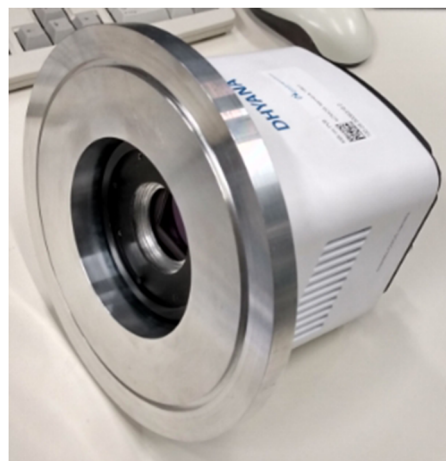


FIG. 1. Photograph of the Tucsen Dhyana 95 sCMOS camera that was modified for the use in the soft x-ray range. The entrance window was removed and an ISO-K 160 vacuum flange was attached.

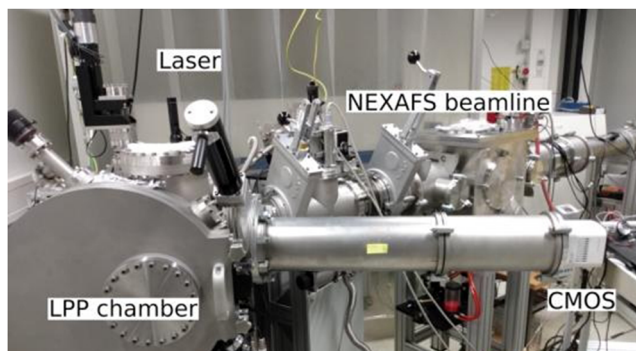


FIG. 2. Photograph of the setup including the Yb:YAG thin disk laser, the LPP chamber, and the two beamlines used for the characterization measurements (front) and the XAFS measurements (back).

residual laser light, the visible part of the emission spectrum and second order diffraction. The dispersed light is collected using either the sCMOS or the CCD detector. The CCD is cooled down to -30°C , and the sCMOS chip is operated at $T = -15^\circ\text{C}$ for all presented measurements. The absorption of the sample is then obtained by the natural logarithm of the incident x-ray spectra divided by the sample spectra. Through the use of multiple pairs of zone plates, all existing absorption edges between 284 eV (C K-edge) and 1303 eV (Mg K-edge) can be measured with a resolving power of $E/\Delta E \geq 900$. The resolving power of the spectrometer at the Ni L-edges amounts to roughly 1000. The whole spectrometer is under high vacuum conditions (10^{-6} mbar).

For the characterization of the sCMOS, the camera was mounted to the chamber in 110 cm distance to the target. The gain was determined using monochromatized radiation and the single photon counting procedure. To attenuate the produced radiation to a photon flux suitable for single photon counting, four layers of aluminum foil of a total thickness of $52\ \mu\text{m}$ were inserted between the target and the detector. The copper plasma emission spectrum convoluted with the transmission of the Al filters results in a mean photon energy of $E_{\text{mean}} = (1440 \pm 30)\ \text{eV}$.

The gain was measured via single photon counting. Frames with 10 ms exposure time were recorded continuously with the LPP at a repetition rate of 100 Hz so that one shot was recorded on each frame on average. 200 frames and 300 dark frames were recorded for each measurement. The median of all dark frames was subtracted, and for each pixel, the standard deviation was calculated. The standard deviation values were then used to determine the noise thresholds for each pixel. The algorithm used to detect photon events on the frames and to assign an intensity value in analog-to-digital units (ADU) was the clustering algorithm described in Ref. 30 with threshold values of $\sigma_1 = 6$ and $\sigma_2 = 3$. To determine an accurate result for the camera gain, only one-pixel events were evaluated.

The sCMOS dark current was measured by recording dark frames for exposure times between 1 s and 10 s, with 20 frames for each measuring point. Since the detector shows some regions with unusually high dark current at the edges of the chip, only a section of the total frames was evaluated to avoid distortion of the results. This value can be seen as a lower limit for the dark current, while

an upper limit is provided by evaluating the whole frame. The mean values of the selected region were plotted over exposure time and the dark current was obtained from the slope of the linear fit. The actual fit error was slightly raised to one significant digit to account for possible small temperature fluctuations.

The readout noise was measured by taking five times 500 dark frames with $20\ \mu\text{s}$ exposure time each, so that the dark noise is negligible. The standard deviation from 500 dark frames was calculated for each pixel and averaged for the whole frame. For the five measurement series, the mean value was calculated. Since the standard errors for both HG and HDR modes are smaller than the difference of both mean values, the errors were estimated on the basis of this difference.

The noise contribution originating from differing offset values of the pixels, the dark signal non-uniformity (DSNU), was measured with the same set of dark frames. For each set of 500 dark frames, the mean value for each pixel was calculated and from those values the DSNU was determined by calculating the standard deviation of the mean pixel values and subtracting the temporal noise. This step was repeated for each set of 500 frames, and the mean value and the standard error were calculated from the five sets. Prior measurements have shown differing values outside of the calculated error range, so a greater error was estimated based on the difference of the results.

For measuring the gain dependent part of the overall noise originating from the different gain characteristics of the readout amplifiers (pixel response non-uniformity, PRNU), flat field frames are necessary, where the sCMOS chip is homogeneously illuminated to investigate the different pixel responses. As a simple alternative to an Ulbricht sphere, a gooseneck lamp combined with a pinhole as the source of homogeneous illumination in the visible range was used for the flat field frames. Frames were recorded for exposure times between 100 ms (10% saturation) and 250 ms (50% saturation) in 50 ms steps in the HDR mode. For every measuring point, 500 flat field frames in addition to 250 dark frames were taken, which were averaged and subtracted from the flat field frames to mitigate the DSNU. The relative PRNU was estimated by dividing the frame standard deviation by the mean frame value. A homogeneous part of the frame was chosen to obtain a lower estimate for the PRNU, while the whole frame was evaluated for an upper estimate (assuming some degree of non-uniformity in the illumination). The mean values of the four measuring points were calculated. For the operation of the sCMOS camera, the manufacturer's software Mosaic 1.6.1 was used.

C. Samples

For the XAFS measurements, a Ni sample has been fabricated by resistive thermal evaporation at the nanoscale lab of the Max-Born-Institute (MBI). The sample consists of a thin Ni layer with a thickness of 100 nm on top of a 150 nm thick Si_3N_4 window with a size of $3 \times 3\ \text{mm}^2$.

As another example, a sandwich sample consisting of three layers (TiO_2 on Au-nanoparticles on NiO) was measured at the Ni L-edges. The exact layer thicknesses are unknown but it is expected that they amount to some tens of nanometers. The sample was prepared on a 150 nm thick, $1 \times 2\ \text{mm}^2$ Si_3N_4 window. The sample system finds application as a plasmonic solar cell prototype device.^{31,32}

TABLE I. Measured noise values and dark current for the Tucsen Dhyana 95 sCMOS camera compared with the manufacturer's values.

	Measured value	Manufacturer's value
Dark current/e ⁻ /s	Lower limit:	1.5 @ T = -10 °C ³⁴
	0.9 ± 0.1 @ T = -15 °C, HDR	1.0 @ T = -20 °C (CCD)
	0.9 ± 0.1 @ T = -15 °C, HG	
	Upper limit:	
	1.1 ± 0.1 @ T = -15 °C, HDR	
Readout noise/e ⁻	1.1 ± 0.1 @ T = -15 °C, HG	
	1.81 ± 0.02, HDR	1.45 ³⁴
	1.79 ± 0.02, HG	8.5 @ 1 MHz (CCD)
Dark signal non-uniformity (DSNU)/e ⁻	0.38 ± 0.05	N/A
Pixel response non-uniformity (PRNU)/%	Lower limit: 0.7 (x: 220–1460, y: 593–1508)	N/A
	Upper limit: 2.7 (full frame)	

III. RESULTS

A. Characterization measurements

The sCMOS detector was characterized regarding its dark current, readout noise, DSNU, and the PRNU with visible light. For both gain modes (HDR and HG), the results of these measurements are shown in Table I. The results are in accordance with the manufacturer's values and show that the dark and readout noise levels of the sCMOS detector are superior to a conventional soft x-ray CCD detector.²⁸ The gain for the HDR mode was calculated to be $g_{\text{HDR}} = (0.52 \pm 0.01) \text{ e}^-/\text{ADU}$ and for the HG mode, $g_{\text{HG}} = (0.03 \pm 0.01) \text{ e}^-/\text{ADU}$. The errors are estimated by assuming an error for the determination of the mean photon energy of $\Delta E_{\text{ph}} = 30 \text{ eV}$. As the average number of electrons per eV, the value of 3.65 eV/e^- ³³ was used.

B. XAFS measurements

For the XAFS measurement, the sCMOS camera was triggered by the LPP source with 100 Hz. 20 000 images were taken. To achieve the desired 100 Hz frame rate, only a region of interest (ROI) consisting of 460 out of the 2048 rows was read out. The limited size of the ROI has no effect on the XAFS spectra other than reducing the measured energy range to $\sim 50 \text{ eV}$, which is more than sufficient for the investigation of the Ni L₃ and L₂ edges simultaneously. To minimize the effect of the DSNU on the XAFS spectrum, the camera was oriented so that the directions of the readout and dispersion are equal. The camera is connected to a personal computer (PC) via universal serial bus (USB) 3.0. The data can be stored on a hard disk drive (HDD) or temporarily in the random-access memory (RAM). Each tiff image with $460 \times 1344 \text{ pixels}^2$ has a size of 1.21 MB. Due to the use of a conventional non-optimized personal computer with 4 GB RAM and a HDD, the data could not be saved at 100 fps and the 20 000 images had to be taken in 20 stacks of 1000 images. Each 1000 image stack was acquired with a frame rate of 100 fps. After recording a stack, the 1.21 GB of data were transferred from the RAM to the HDD, which took about 20 s. Therefore, the actual acquisition time for the 20 000 images was about 10 min, which translates to 33 Hz acquisition rate. Using dedicated hardware, data accumulation with 100 Hz is possible continuously. For the XAFS measurement with the CCD detector, 1000 single

shot images were collected with $8 \times$ binning, resulting in a 0.5 Hz frame rate. The total measuring time was 33 min. The data processing procedure to evaluate the XAFS spectrum is explained in detail in Ref. 22.

Figure 3 shows the XAFS spectra of the nickel sample measured with the CCD (black) and sCMOS detector. For both measurements, the LPP is operated with 100 mJ pulse energy and 1 ns pulse duration. Tungsten was used as the plasma target material. The spectrum was energy calibrated using a reference spectrum.³⁵ The resolving power has been estimated to be around 1000. The spectra show four distinct features. Starting from low energies, the first peak corresponds to the Ni L₃-edge ($2p_{3/2}$ to $3d$). The third peak corresponds to the Ni L₂-edge absorption ($2p_{1/2}$ to $3d$). The second (858 eV)

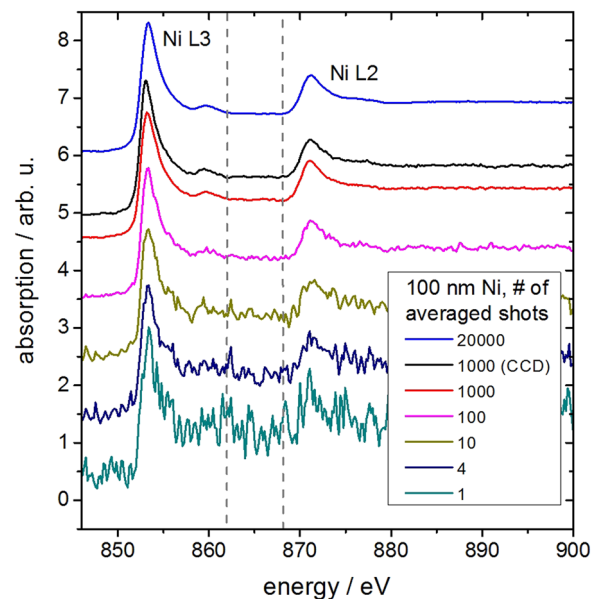


FIG. 3. XAFS spectra of a 100 nm thick Ni foil at the Ni L₃ and L₂ edges measured with a CCD and sCMOS camera for direct comparison. Measurement times were 10 min (20 000 images) and 30 s (1000 images) for the sCMOS and 33 min for the CCD detector (for 1000 images). The spectra are displayed with an offset.

and fourth (877 eV) weaker features are related to the density of state effects discussed in Refs. 35 and 36.

To investigate the feasibility of QXAFS measurements, the spectra derived from different numbers of averaged shots are shown. Using 100 Hz, one XAFS spectrum is generated every 10 ms. If a lower statistical error is needed for a given application, multiple images can be averaged at the cost of time resolution. Averaging over multiple images increases the quality of the XAFS by the square root of the number of images taken. Table II summarizes the values for selected parameters. If the full frame of the CMOS would be necessary, a time resolution of about 40 ms can be reached, resulting in a standard deviation of 0.128.

To compare the absolute statistical error of the sCMOS and the CCD measurement, the standard deviation of the signal in the region between 862 eV and 868 eV was used, which corresponds to 29 pixels and a channel width of 0.21 eV for the CCD and 34 px and 0.18 eV for the sCMOS. The region is marked with gray dashed vertical lines in Fig. 3 and was flattened using a linear fit prior calculating the standard deviation. The standard deviation of one single shot image is 0.280 for the CCD and 0.248 for the sCMOS camera. After averaging over 1000 images, the statistical error is reduced to 0.009 for the CCD measurement and 0.009 for the sCMOS measurement. After 20 000 images, the statistical error of the sCMOS measurement is reduced to 0.004. While for the CCD measurement the statistical error is in good agreement with the Poisson limit,²² the sCMOS measurement shows an offset of >0.002. This is presumably due to PRNU. The effect of the PRNU in the XAFS spectrum is smaller than the value given in Table I because of averaging processes. At 1000 images, using the full repetition rate and high readout speed of the sCMOS camera, the quality of the XAFS spectrum is very similar to the CCD but at only 1/66 of measurement time.

As an example for the merits of fast acquisition possibilities, in general, a more complex layered sample was measured. The XAFS spectrum is depicted in Fig. 4.

The TiO₂/Au-nanoparticle/NiO sample contains approximately one order of magnitude less nickel than the pure Ni sample on a 4.5 times smaller sample area. While the exact NiO layer thickness is unknown, the absolute absorption values suggest a thickness of about 30 nm, of which only half is nickel. 50 000 images were taken with the sCMOS in 25 min and evaluated. The statistics follow the same pattern as the Ni measurement. The standard deviation of one single shot image is about 0.45. After 50 000 images, a standard deviation of 0.004 was determined. Again, an offset of 0.002 larger than pure Poisson statistics can be seen.

TABLE II. Summary of the different possible QXAFS scenarios with the corresponding time resolution and standard deviation of the XAFS spectrum using the sCMOS detector.

Number of avg. shots	Time resolution	Standard deviation
1	10 ms (0.5 s CCD)	0.248, (0.280 CCD)
4	40 ms	0.128
10	100 ms	0.070
100	1 s	0.022
1000	10 s (33 min CCD)	0.009, (0.009 CCD)
20 000	200 s	0.004

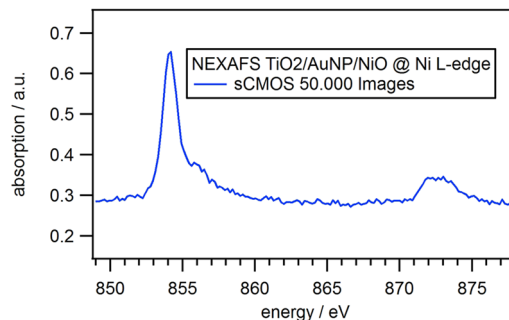


FIG. 4. XAFS spectrum at the Ni L-edges of a sample containing a TiO₂, an Au nanoparticle, and a NiO layer.

The spectrum shows a 5 times higher relative error than the Ni spectrum (cp. Fig. 3), but most features can be discerned. The L₂- and L₃-edge each split into t_{2g} and e_g orbitals, but only the transitions into the e_g orbital can be seen because the t_{2g} orbital is fully occupied in the ground state. The L₃-edge is further split due to multiplet effects. A detailed description of the features and NiO reference spectra can be found in Refs. 37 and 38.

IV. DISCUSSION AND OUTLOOK

A commercially available sCMOS camera intended for the visible light range was successfully adapted to investigations using soft x-ray radiation. As an application, XAFS measurements of a 100 nm thin nickel film with a laboratory LPP source were selected, where the readout time of the detector, a commercial x-ray CCD camera, was up until now the limiting factor for fast data acquisition. The measurement time could be reduced drastically by a factor of 66, possibly 200, when using dedicated hardware for data acquisition in the future. Successive XAS measurements with 100 Hz repetition rate could be realized. The fast data acquisition rate of the sCMOS renders laboratory QXAFS measurements with a time resolution of down to 10 ms possible, which is comparable to the state of the art QXAFS beamlines at synchrotron radiation facilities.^{3,4,7,9} Depending on the time scale and the requirement for statistical certainty of the measurement, the number of averaged images can be adjusted. A statistical analysis of the XAFS spectra shows that an offset of the statistical error of about 0.002 exists in each XAFS spectrum taken with the sCMOS, which is most probably due to the pixel response non-uniformity. With a good calibration using more elaborate flat field measurements than those used in this work, this noise source can possibly be eliminated. With the current sample chamber, QXAFS measurements of thermal processes by heating the sample can be performed.¹¹ Using dedicated sample chambers, thin film growth processes can be investigated.¹⁰ By adapting gas or liquid transmission flow cells to this setup, gas-solid or liquid-solid catalytic reactions can be studied in the laboratory.¹² Regarding time consuming pump-probe XAFS, changes in absorption of <10⁻³ can be detected, rendering measurements feasible in less than one day compared to weeks using CCD technology. A XAFS spectrum, consisting of 50 000 averaged single shot spectra, on a complex sandwich structure with minute amounts of NiO was shown. This presents an example, where a high frame rate is mandatory for adequate

statistics in reasonable measurement time scales. Taking 50 000 images with the CCD detector would take 28 h.

sCMOS technology shows great potential for replacing CCDs in ultrafast x-ray science, especially due to their superior frame rate. However, the absence of dedicated sCMOS cameras for the (soft) x-ray range makes adaption such as removal of windows and vacuum integration necessary for now. For future experiments, improved software and detector functionality may enable the simultaneous readout of specific parts of the frame or the reduction of the pixel depth to 12 bit, thus improving the frame rate and reducing the frame file size. The used version of the Dhyana does not allow measurements with 12 bit pixel depth, although it is in principle possible with the GSENSE400BSI.^{26,27} sCMOS sensors with readout electronics in every pixel could improve frame rates and readout flexibility even further, but the complexity of the electronics leading to high noise values combined with a lacking fill factor and quantum efficiency renders the use of such detectors in the x-ray range difficult for now.

ACKNOWLEDGMENTS

This work was conducted in the framework of DFG Project No. 313838950. We thank Dieter Engel and Denny Sommer (MBI) for producing the nickel sample. We thank the working group of Jacinto Sá for providing us with the TiO₂/Au-NP/NiO sample. This work was funded by Deutsche Forschungsgemeinschaft (Grant No. 313838950) and LASERLAB Europe (Grant No. 654148).

The authors declare no conflicts of interest.

DATA AVAILABILITY

The data that support the findings of this study are available from the corresponding author upon reasonable request.

REFERENCES

- ¹R. Frahm, "New method for time dependent x-ray absorption studies," *Rev. Sci. Instrum.* **60**, 2515 (1989).
- ²M. Richwin, R. Zaeper, D. Lützenkirchen-Hecht, and R. Frahm, "Piezo-XAFS—time-resolved x-ray absorption spectroscopy," *Rev. Sci. Instrum.* **73**, 1668 (2002).
- ³T. Nonaka, K. Dohmae, T. Araki, Y. Hayashi, Y. Hirose, T. Uruga, H. Yamazaki, T. Mochizuki, H. Tanida, and S. Goto, "Quick-scanning x-ray absorption spectroscopy system of a servo-motor-driven channel-cut monochromator with a temporal resolution of 10 ms," *Rev. Sci. Instrum.* **83**, 083112 (2012).
- ⁴W. Limphirat, N. Wiriya, S. Tonlublao, S. Chaichoy, P. Pruekthaisong, S. Duandmanee, P. Kamonpha, D. Kaewsuwan, N. Meethong, R. P. Poo-arporn, P. Songsiririthigul, J. Holmes, and Y. Poo-arporn, "The current status of time-resolved XAS beamline at SLRI and application on *in situ* experiments," *Radiat. Phys. Chem.* **171**, 108750 (2020).
- ⁵A. Kulow, S. Witte, S. Beyer, A. Guilherme Buzanich, M. Radtke, U. Reinholz, H. Riesemeier, and C. Strelt, "A new experimental setup for time- and laterally-resolved X-ray absorption fine structure spectroscopy in a 'single shot'," *J. Anal. At. Spectrom.* **34**, 239–246 (2019).
- ⁶S. Chu, L. Zheng, P. An, H. Gong, T. Hu, Y. Xie, and J. Zhang, "Time-resolved XAFS measurement using quick-scanning techniques at BSRF," *J. Synchrotron Radiat.* **24**, 674–679 (2017).
- ⁷O. Müller, M. Nachtegaal, J. Just, D. Lützenkirchen-Hecht, and R. Frahm, "Quick-EXAFS setup at the SuperXAS beamline for *in situ* X-ray absorption spectroscopy with 10 ms time resolution," *J. Synchrotron Radiat.* **23**, 260–266 (2016).
- ⁸A. H. Clark, P. Steiger, B. Bornmann, S. Hitz, R. Frahm, D. Ferri, and M. Nachtegaal, "Fluorescence-detected quick-scanning X-ray absorption spectroscopy," *J. Synchrotron Radiat.* **27**, 681–688 (2020).
- ⁹B. Bornmann, J. Kläs, O. Müller, D. Lützenkirchen-Hecht, and R. Frahm, "The quick EXAFS setup at beamline P64 at PETRA III for up to 200 spectra per second," *AIP Conf. Proc.* **2054**, 040008 (2019).
- ¹⁰D. Lützenkirchen-Hecht, J. Stötzl, O. Müller, J. Just, and R. Frahm, "Quick-Scanning QEXAFS in grazing incidence: Surface science in sub-seconds," *J. Phys.: Conf. Ser.* **430**, 012124 (2013).
- ¹¹M. Scholz, F. Holch, C. Sauer, M. Wiessner, A. Schöll, and F. Reinert, "Core hole-electron correlation in coherently coupled molecules," *Phys. Rev. Lett.* **111**, 048102 (2013).
- ¹²H. Yuzawa, M. Nagasaka, and N. Kosugi, "*In situ* soft X-ray absorption spectroscopy applied to Solid-Liquid heterogeneous cyanopyrazine hydration reaction on titanium oxide catalyst," *J. Phys. Chem. C* **119**, 7738–7745 (2015).
- ¹³R. Geneaux, H. J. B. Marroux, A. Guggenmos, D. M. Neumark, and S. R. Leone, "Transient absorption spectroscopy using high harmonic generation: A review of ultrafast X-ray dynamics in molecules and solids," *Philos. Trans. R. Soc. A* **377**, 20170463 (2019).
- ¹⁴J. Weissaupt, A. Rouzée, M. Woerner, M. J. J. Vrakking, T. Elsaesser, E. L. Shirley, and A. Borgschulte, "Ultrafast modulation of electronic structure by coherent phonon excitations," *Phys. Rev. B* **95**, 081101 (2017).
- ¹⁵E. S. Ryland, M.-F. Lin, M. A. Verkamp, K. Zhang, K. Benke, M. Carlson, and J. Vura-Weis, "Tabletop femtosecond M-edge X-ray absorption near-edge structure of FeTPPCL: Metalloporphyrin photophysics from the perspective of the metal," *J. Am. Chem. Soc.* **140**, 4691–4696 (2018).
- ¹⁶S. L. Cousin, F. Silva, S. Teichmann, M. Hemmer, B. Buades, and J. Biegert, "High-flux table-top soft x-ray source driven by sub-2-cycle, CEP stable, 1.85-μm 1-kHz pulses for carbon K-edge spectroscopy," *Opt. Lett.* **39**, 5383–5386 (2014).
- ¹⁷D. Popmintchev, B. R. Galloway, M.-C. Chen, F. Dollar, C. A. Mancuso, A. Han-klä, L. Miaja-Avila, G. O'Neil, J. M. Shaw, G. Fan, S. Ališauskas, G. Andriukaitis, T. Balčiunas, O. D. Mücke, A. Pugzlys, A. Baltuška, H. C. Kapteyn, T. Popmintchev, and M. M. Murnane, "Near- and extended-edge X-ray-absorption fine-structure spectroscopy using ultrafast coherent high-order harmonic supercontinua," *Phys. Rev. Lett.* **120**, 093002 (2018).
- ¹⁸C. Kleine, M. Ekimova, G. Goldsztejn, S. Raabe, C. Strüber, J. Ludwig, S. Yarlagadda, S. Eisebitt, M. J. J. Vrakking, T. Elsaesser, E. T. J. Nibbering, and A. Rouzée, "Soft X-ray absorption spectroscopy of aqueous solutions using a table-top femtosecond soft X-ray source," *J. Phys. Chem. Lett.* **10**, 52–58 (2019).
- ¹⁹I. Mantouvalou, K. Witte, W. Martyanov, A. Jonas, D. Grötzsch, C. Streeck, H. Löchel, I. Rudolph, A. Erko, H. Stiel, and B. Kannigieser, "Single shot near edge x-ray absorption fine structure spectroscopy in the laboratory," *Appl. Phys. Lett.* **108**, 201106 (2016).
- ²⁰M. Müller, M. Schellhorn, and K. Mann, "Laboratory-scale near-edge X-ray absorption fine structure spectroscopy with a laser-induced plasma source," *J. Anal. At. Spectrom.* **34**, 1779–1785 (2019).
- ²¹P. Wachulak, M. Duda, A. Bartnik, A. Sarzyński, Ł. Węgrzyński, M. Nowak, A. Jancarek, and H. Fiedorowicz, "Compact system for near edge X-ray fine structure (NEXAFS) spectroscopy using a laser-plasma light source," *Opt. Express* **26**, 8260–8274 (2018).
- ²²A. Jonas, H. Stiel, L. Glöggler, D. Dahm, K. Dammer, B. Kannigieser, and I. Mantouvalou, "Towards Poisson limited optical pump soft X-ray probe NEXAFS spectroscopy using a laser-produced plasma source," *Opt. Express* **27**, 36524–36537 (2019).
- ²³M. Bigas, E. Cabruja, J. Forest, and J. Salvi, "Review of CMOS image sensors," *Microelectron. J.* **37**, 433–451 (2006).
- ²⁴W. X. Wang, Z. X. Ling, C. Zhang, Z. Q. Jia, X. Y. Wang, Q. Wu, W. M. Yuan, and S. N. Zhang, "Characterization of a BSI sCMOS for soft X-ray imaging spectroscopy," *J. Instrum.* **14**, P02025 (2019).
- ²⁵K. Desjardins, H. Popescu, P. Mercère, C. Meneglier, R. Gaudemer, K. Thänell, and N. Jaouen, "Characterization of a back-illuminated CMOS Camera for soft x-ray coherent scattering," *AIP Conf. Proc.* **2054**, 060066 (2019).

- ²⁶T. Harada, N. Teranishi, T. Watanabe, Q. Zhou, X. Yang, J. Bogaerts, and X. Wang, "Energy- and spatial-resolved detection using a backside-illuminated CMOS sensor in the soft X-ray region," *Appl. Phys. Express* **12**, 082012 (2019).
- ²⁷N. Narukage, S.-n. Ishikawa, T. Sakao, and X. Wang, "High-speed back-illuminated CMOS sensor for photon-counting-type imaging-spectroscopy in the soft X-ray range," *Nucl. Instrum. Methods Phys. Res., Sect. A* **950**, 162974 (2020).
- ²⁸Greateyes GmbH, <https://www.greateyes.de>.
- ²⁹I. Mantouvalou, K. Witte, D. Grötzsch, M. Neitzel, S. Günther, J. Baumann, R. Jung, H. Stiel, B. Kanngießer, and W. Sandner, "High average power, highly brilliant laser-produced plasma source for soft X-ray spectroscopy," *Rev. Sci. Instrum.* **86**, 035116 (2015).
- ³⁰J. Baumann, R. Gnewkow, S. Staack, V. Szwedowski-Rammert, C. Schlesiger, I. Mantouvalou, and B. Kanngießer, "Photon event evaluation for conventional pixelated detectors in energy-dispersive X-ray applications," *J. Anal. At. Spectrom.* **33**, 2043–2052 (2018).
- ³¹Y. Hattori, M. Abdellah, J. Meng, K. Zheng, and J. Sá, "Simultaneous hot electron and hole injection upon excitation of gold surface plasmon," *J. Phys. Chem. Lett.* **10**, 3140–3146 (2019).
- ³²K. Nakamura, T. Oshikiri, K. Ueno, Y. Wang, Y. Kamata, Y. Kotake, and H. Misawa, "Properties of plasmon-induced photoelectric conversion on a TiO₂/NiO p–n junction with Au nanoparticles," *J. Phys. Chem. Lett.* **7**, 1004–1009 (2016).
- ³³M. N. Mazziotta, "Electron-hole pair creation energy and Fano factor temperature dependence in silicon," *Nucl. Instrum. Methods Phys. Res., Sect. A* **584**, 436–439 (2008).
- ³⁴Tucsen Photonics, <http://www.tucsen.com/en.html>.
- ³⁵Y. Ufuktepe, G. Akgül, F. Aksoy, and D. Nordlund, "Thickness and angular dependence of the L-edge X-ray absorption of nickel thin films," *X-Ray Spectrom.* **40**, 427–431 (2011).
- ³⁶J. Fink, T. Müller-Heinzerling, B. Scheerer, W. Speier, F. U. Hillebrecht, J. C. Fuggle, J. Zaanen, and G. A. Sawatzky, "2p absorption spectra of the 3d elements," *Phys. Rev. B* **32**, 4899–4904 (1985).
- ³⁷H. Ikeno, I. Tanaka, Y. Koyama, T. Mizoguchi, and K. Ogasawara, "First-principles multielectron calculations of Ni L_{2,3} NEXAFS and ELNES for LiNiO₂ and related compounds," *Phys. Rev. B* **72**, 075123 (2005).
- ³⁸K. Ogasawara, T. Iwata, Y. Koyama, T. Ishii, I. Tanaka, and H. Adachi, "Relativistic cluster calculation of ligand-field multiplet effects on cation L_{2,3} X-ray-absorption edges of SrTiO₃, NiO, and CaF₂," *Phys. Rev. B* **64**, 115413 (2001).